



**HAL**  
open science

## Microreactors to Measure Solubilities in the CO<sub>2</sub>-H<sub>2</sub>O-NaCl System

Marie-Camille Caumon, Jean Dubessy, Pascal Robert, Boubaker Benaissa

► **To cite this version:**

Marie-Camille Caumon, Jean Dubessy, Pascal Robert, Boubaker Benaissa. Microreactors to Measure Solubilities in the CO<sub>2</sub>-H<sub>2</sub>O-NaCl System. 13th International Conference on Greenhouse Gas Control Technologies, GHGT-13, Nov 2017, Lausanne, Switzerland. pp.4843-4850, 10.1016/j.egypro.2017.03.1624 . hal-01575637

**HAL Id: hal-01575637**

**<https://hal.science/hal-01575637v1>**

Submitted on 23 Aug 2017

**HAL** is a multi-disciplinary open access archive for the deposit and dissemination of scientific research documents, whether they are published or not. The documents may come from teaching and research institutions in France or abroad, or from public or private research centers.

L'archive ouverte pluridisciplinaire **HAL**, est destinée au dépôt et à la diffusion de documents scientifiques de niveau recherche, publiés ou non, émanant des établissements d'enseignement et de recherche français ou étrangers, des laboratoires publics ou privés.



13th International Conference on Greenhouse Gas Control Technologies, GHGT-13, 14-18  
November 2016, Lausanne, Switzerland

## Microreactors to measure solubilities in the CO<sub>2</sub>-H<sub>2</sub>O-NaCl system

Marie-Camille Caumon<sup>a\*</sup>, Jean Dubessy<sup>a</sup>, Pascal Robert<sup>a</sup>, Boubaker Benaissa<sup>a</sup>

<sup>a</sup>Université de Lorraine, CNRS, CREGU, GeoRessources laboratory, BP 70239, F-54506 Vandœuvre-lès-Nancy, France

### Abstract

The production of experimental data for CO<sub>2</sub> solubilities in the H<sub>2</sub>O-CO<sub>2</sub>-NaCl is of first importance to constraint thermodynamic modelling of CO<sub>2</sub> geological storage. Here a microcapillaries device is coupled to a Raman microspectrometer to measure CO<sub>2</sub> solubility as a function of pressure, temperature and NaCl concentration. The results show an excellent correlation with the equation of state of Duan and Sun [1] and with previous works [2].

© 2017 The Authors. Published by Elsevier Ltd. This is an open access article under the CC BY-NC-ND license (<http://creativecommons.org/licenses/by-nc-nd/4.0/>).

Peer-review under responsibility of the organizing committee of GHGT-13.

*Keywords:* CO<sub>2</sub> solubility; Raman spectroscopy, fused silica micro-reactor

### 1. Introduction

The knowledge of the solubility of CO<sub>2</sub> in water and saline solutions is crucial to model the behavior of CO<sub>2</sub> after injection in an aquifer for CO<sub>2</sub> storage purpose. Over the last decades, numerous experimental data have been acquired, mostly at low pressure (< 200 bar, Fig. 1) and in pure water but data at higher pressure or in saline media are sparse. In the present study, a micro-reactor was used, coupled with a Raman microspectrometer to measure solubilities in the CO<sub>2</sub>-H<sub>2</sub>O-NaCl system. The optical device made possible to measure CO<sub>2</sub>/H<sub>2</sub>O concentrations without sampling, i.e. without perturbation of the system after calibration. Moreover, the micro-reactor reduced equilibration times and heat and mass transfers contrary to classical batch reactor [3].

\* Corresponding author. Tel.: +33 3 83 68 47 25; fax: +33 3 83 68 47 01.  
E-mail address: [marie-camille.caumon@univ-lorraine.fr](mailto:marie-camille.caumon@univ-lorraine.fr)

The objective of this study was to define the relevant parameters to be used to draw calibration curves correlating the dissolved CO<sub>2</sub> concentration with the Raman signal of CO<sub>2</sub> and H<sub>2</sub>O at any salinity and temperature. The Raman signal of CO<sub>2</sub> and water were acquired as a function of pressure, temperature and NaCl concentration. The ranges were 5-500 bar, 25-250 °C, and 0-4 M NaCl. The peak areas (A) and peak intensities (I) were measured for the HOH bending vibration (~1640 cm<sup>-1</sup>, noted b) and the OH stretching vibration (~3350 cm<sup>-1</sup>, noted s) of H<sub>2</sub>O, and for the Fermi doublet of CO<sub>2</sub> (both peaks or only the v<sup>+</sup> peak at ~1380 cm<sup>-1</sup>). The following peak intensity and area ratios were plotted as a function of CO<sub>2</sub> solubility:  $A_{CO_2}/A_{H_2O_s}$ ,  $A_{CO_2}/A_{H_2O_b}$ ,  $A_{CO_2-1380}/A_{H_2O_s}$ ,  $A_{CO_2-1380}/A_{H_2O_b}$ ,  $I_{CO_2-1380}/I_{H_2O_s}$ , and  $I_{CO_2-1380}/I_{H_2O_b}$ . The CO<sub>2</sub> solubility was calculated using the model of Duan and Sun [1] at the pressure and temperature of each step.

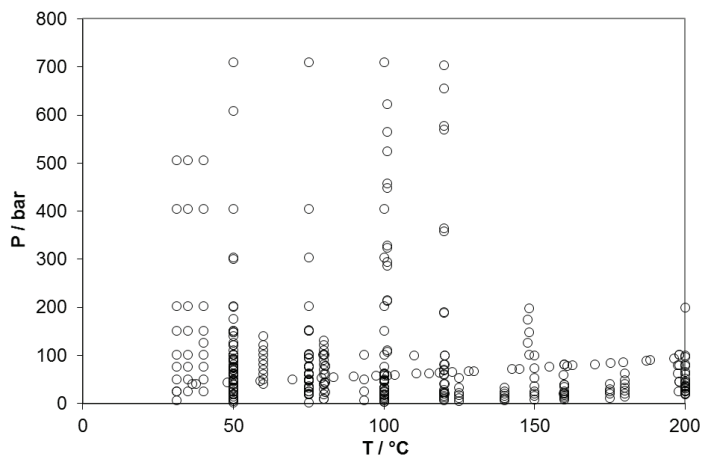


Fig. 1: literature review of the *PT* conditions of CO<sub>2</sub> solubility data in H<sub>2</sub>O.

### Nomenclature

$A_{CO_2}$	Area of the v <sup>+</sup> and v <sup>-</sup> Raman peaks of CO <sub>2</sub> (1380 and 1273 cm <sup>-1</sup> )
$A_{CO_2-1380}$	Area of the v <sup>+</sup> Raman peak of CO <sub>2</sub> .
$A_{H_2O_b}$	Area of the bending vibration band of H <sub>2</sub> O (1640 cm <sup>-1</sup> )
$A_{H_2O_s}$	Area of the stretching vibration band of H <sub>2</sub> O (2800-3850 cm <sup>-1</sup> )
$I_{CO_2}$	Intensity of the v <sup>+</sup> Raman peak of CO <sub>2</sub> .
$I_{H_2O_b}$	Intensity of the bending vibration band of H <sub>2</sub> O (1640 cm <sup>-1</sup> )
$I_{H_2O_s}$	Intensity of the stretching vibration band of H <sub>2</sub> O (2800-3800 cm <sup>-1</sup> )
QF	$(I_{CO_2-1380}/I_{H_2O_s})/s_{CO_2}$
$s_{CO_2}$	solubility of CO <sub>2</sub> (mol.kg <sup>-1</sup> H <sub>2</sub> O)

## 2. Material and methods

### 2.1. Experimental device and procedure

The experimental device is a High Pressure Optical Cell (HPOC) [4] which consists of a pressurization system connected to a fused silica capillary tube. The capillary tube is placed on a customized heating-cooling stage (CAP500, Linkam) (Fig. 2). Temperature and pressure measurements were calibrated before experiments. Temperature is

controlled to  $\pm 0.1$  °C. Pressure is controlled to  $\pm 0.3$  bar. Measurements are done at 25 °C in pure water and 1, 2, 3, and 4 M NaCl up to 500 bar, and at 25, 100, 200, and 250 °C in pure water, up to 500 bar. The solubility of CO<sub>2</sub> is calculated at each pressure-temperature- $m_{\text{NaCl}}$  step using the equation of state of Duan and Sun [1].

The fused silica tube is first filled with about 0.5 cm of water or of a NaCl solution. It is then glued to a stainless steel tube and connected to the pressurization device. The solution is frozen and all the system is evacuated under vacuum. A few bars of CO<sub>2</sub> are loaded in the tube before unfreezing the solution. CO<sub>2</sub> is added step by step up to 500 bar. The Raman spectra are acquired near the gas-solution interface once the Raman signal and pressure stabilize.

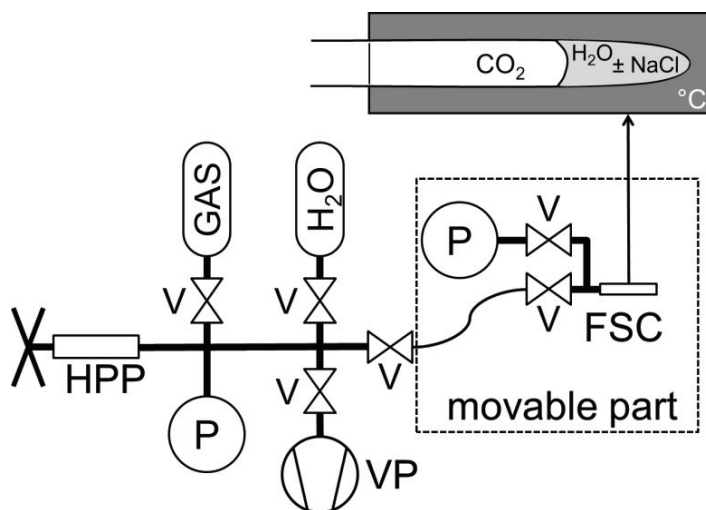


Fig. 2: the HPOC system after Caumon *et al.* [5]. HPP: high pressure pump; P: pressure transducer; V: valve; VP: vacuum pump; FSC: fused silica capsule.

## 2.2. Raman analysis

Raman spectra are recorded using a LabRAM HR microspectrometer (Horiba Jobin Yvon) equipped with a 600  $\text{gr.mm}^{-1}$  grating and an x20 objective (Olympus). The laser is an Ar<sup>+</sup> laser (Stabilite 2017, Spectra-Physics) operating at 514.53 nm and 200 mW. The acquisition time is generally of 10 to 30 s with 10 accumulations. Each measurement is repeated 10 times. Peak areas and intensities are measured using Labspec software (Horiba Jobin Yvon). A straight baseline is subtracted.

## 3. Results and discussion

### 3.1. Raman spectra of dissolved CO<sub>2</sub> and liquid water

Some examples of the Raman spectra of CO<sub>2</sub> and water are presented in Fig. 3. The Raman signal of dissolved CO<sub>2</sub> consists of a doublet at 1273  $\text{cm}^{-1}$  and 1380  $\text{cm}^{-1}$  (Fig. 3a). The Raman signal of water is presented here as the bending vibration band around 1640  $\text{cm}^{-1}$  (Fig. 3a) and the stretching vibration band in the range 2800-3800  $\text{cm}^{-1}$  (Fig. 3b). The Raman signal of dissolved CO<sub>2</sub> only changes in intensity with concentration. On the contrary, the shape of the Raman vibration bands of water evolves with salinity (Fig. 3a and Fig. 3b), pressure, and temperature, especially the stretching vibration band around 3500  $\text{cm}^{-1}$ . This modification is due to changes in hydrogen bonding between H<sub>2</sub>O molecules in liquid water and is widely discussed in literature (e.g. [6] and ref. therein).

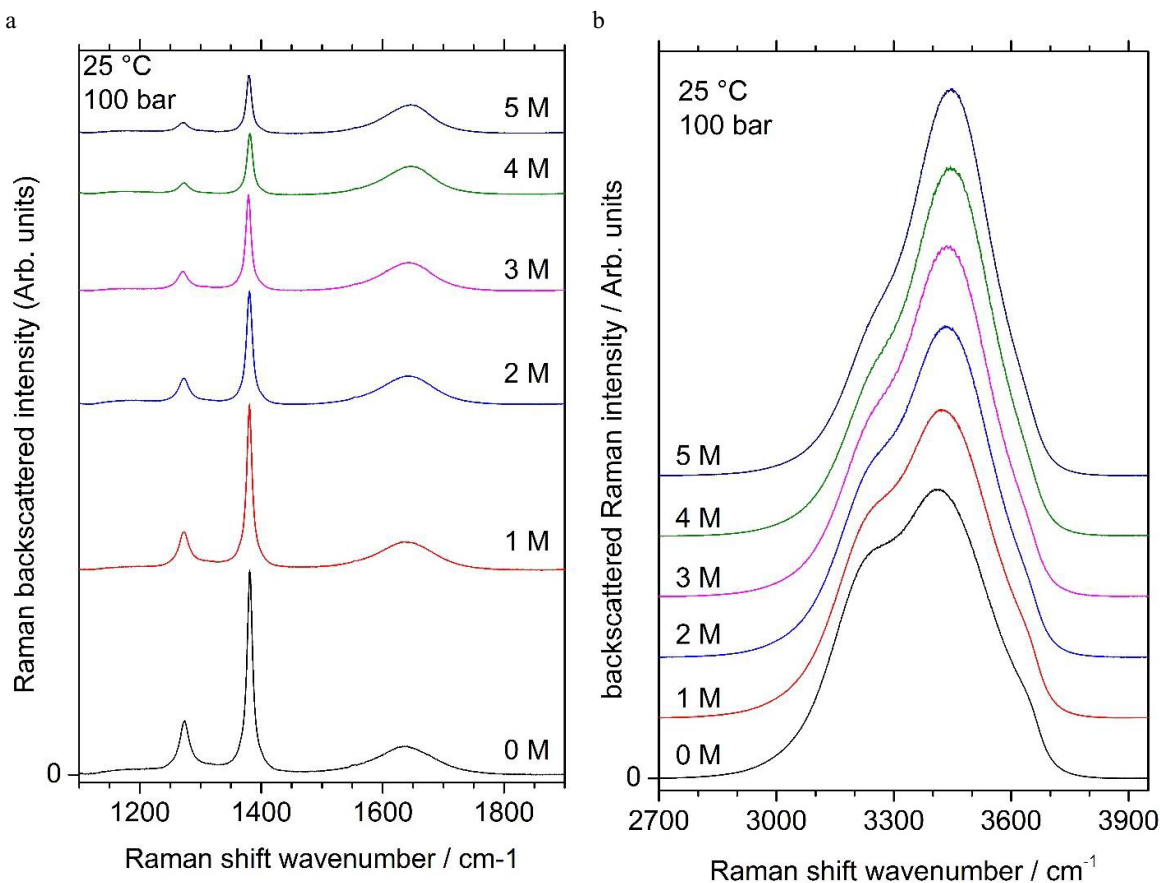


Fig. 3: Some Raman spectra of (a) dissolved CO<sub>2</sub> and the bending vibration band of water and (b) the stretching vibration band of water, as a function of NaCl concentration. P = 100 bar, T = 25 °C. Spectra are normalized to the area of the bending (a) or stretching (b) band of water and Y-shifted for clarity.

### 3.2. Effect of salinity

Raman spectra of dissolved CO<sub>2</sub> and water were recorded at 25 °C at various salinity (0-4 M NaCl) and pressure up to 500 bar. The effect of salinity is presented in Fig. 4. Six different ratios are calculated and plotted as a function of CO<sub>2</sub> solubility (mol.kg<sup>-1</sup>H<sub>2</sub>O) and salinity (NaCl molality, mol.kg<sup>-1</sup>H<sub>2</sub>O):  $A_{CO_2}/A_{H_2O_b}$  (Fig. 4a),  $A_{CO_2}/A_{H_2O_s}$  (Fig. 4b),  $A_{CO_2-1380}/A_{H_2O_b}$  (Fig. 4c),  $A_{CO_2-1380}/A_{H_2O_s}$  (Fig. 4d),  $I_{CO_2}/I_{H_2O_b}$  (Fig. 4e), and  $I_{CO_2}/I_{H_2O_s}$  (Fig. 4f). A linear regression line is calculated for each data set (fixed intercept = 0). All data sets yield a satisfactory correlation between Raman peak ratios and CO<sub>2</sub> solubility, with a R<sup>2</sup> better than 0.98. Salinity affects the slope of the correlation line in all cases, with various intensity (Fig. 5). The ratio calculated to the bending vibration band of water are more sensitive to salinity than the one calculated to the stretching band water. The less sensitive to salinity is  $A_{CO_2-1380}/A_{H_2O_s}$ . The most sensitive to salinity is  $A_{CO_2}/A_{H_2O_b}$ .

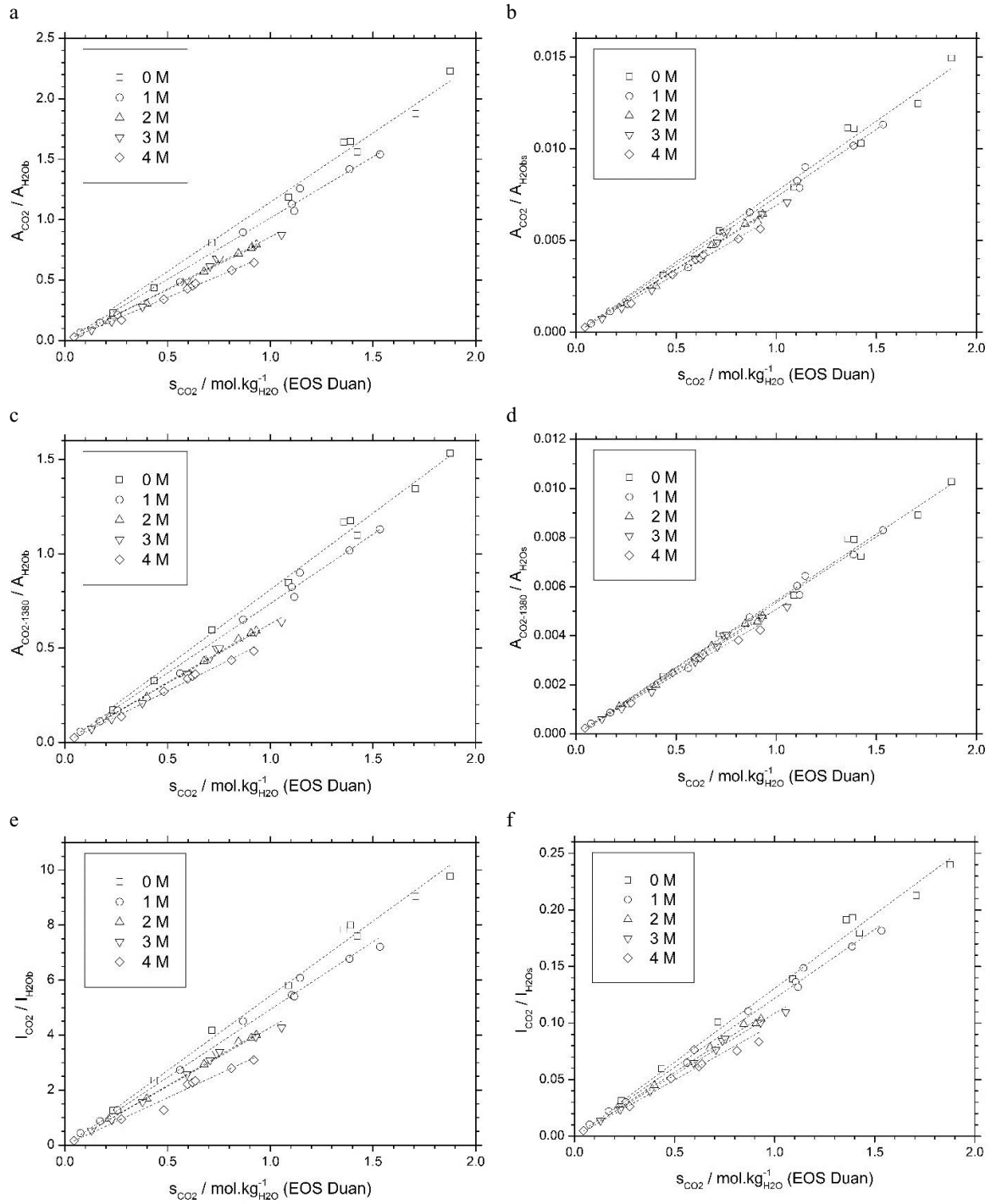


Fig. 4: peak area and peak intensity ratios as a function CO<sub>2</sub> solubility and NaCl concentration (M, mol.kg<sup>-1</sup>H<sub>2</sub>O). (a)  $A_{\text{CO}_2}/A_{\text{H}_2\text{O}b}$ , (b)  $A_{\text{CO}_2}/A_{\text{H}_2\text{O}s}$ , (c)  $A_{\text{CO}_2-1380}/A_{\text{H}_2\text{O}b}$ , (d)  $A_{\text{CO}_2-1380}/A_{\text{H}_2\text{O}s}$ , (e)  $I_{\text{CO}_2}/I_{\text{H}_2\text{O}b}$ , (f)  $I_{\text{CO}_2}/I_{\text{H}_2\text{O}s}$ . Temperature: 25 °C; pressure: 3-500 bar.

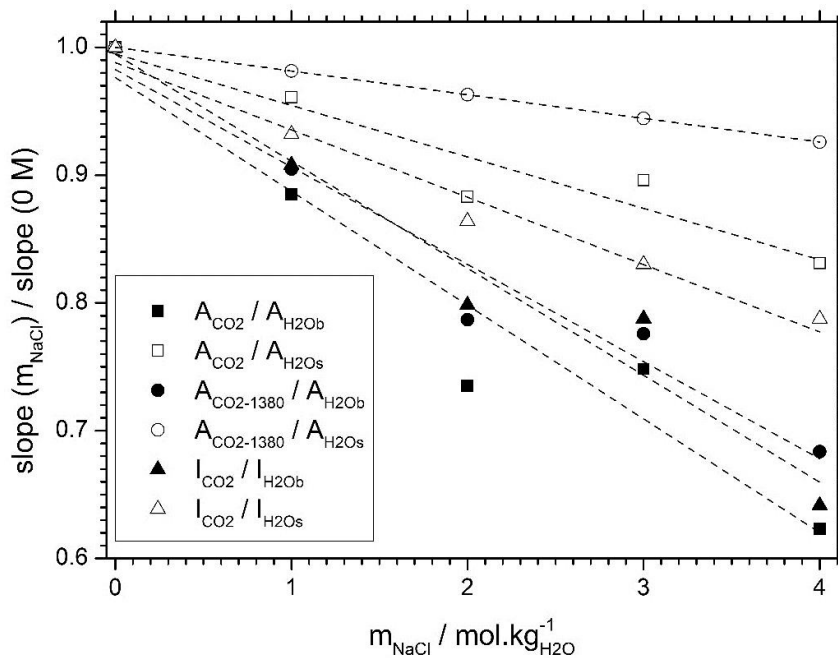


Fig. 5: evolution of the slope of the correlation curves in Fig. 4 with salinity, after normalization to the slope in pure water.

### 3.3. Effect of temperature

Raman spectra of dissolved CO<sub>2</sub> and water were recorded at four different temperatures (25, 100, 200, 250 °C) at pressure up to 500 bar. The same peak area and intensity ratios are calculated and plotted in Fig. 6:  $A_{\text{CO}_2}/A_{\text{H}_2\text{O}b}$  (Fig. 6a),  $A_{\text{CO}_2}/A_{\text{H}_2\text{O}s}$  (Fig. 6b),  $A_{\text{CO}_2-1380}/A_{\text{H}_2\text{O}b}$  (Fig. 6c),  $A_{\text{CO}_2-1380}/A_{\text{H}_2\text{O}s}$  (Fig. 6d),  $I_{\text{CO}_2}/I_{\text{H}_2\text{O}b}$  (Fig. 6e), and  $I_{\text{CO}_2}/I_{\text{H}_2\text{O}s}$  (Fig. 6f). A linear regression line is calculated for each data set (fixed intercept = 0). As the data set at 250 °C has only two data points, this correlation must be carefully considered.

The effect of temperature on the correlation between Raman peak ratios and temperature is weak between 25°C and 100 °C but becomes intense at 200 and 250 °C. The only ratio that remains coherent over the whole temperature range is  $I_{\text{CO}_2} / I_{\text{H}_2\text{O}s}$ . This discrepancy between ratios might be due to a slow evaporation of the liquid phase, and so leads to difficulty to reach equilibrium.

The  $I_{\text{CO}_2} / I_{\text{H}_2\text{O}s}$  ratio, normalized to CO<sub>2</sub> molality (QF), is plotted as a function of temperature, and compared to the data of Guo et al. [2] (Fig. 7). Despite a small shift of our data toward higher values, the trend is very similar. The difference between the two data sets may be due to a difference of baseline subtraction, of the spectrometer response, or in equilibrium procedures.

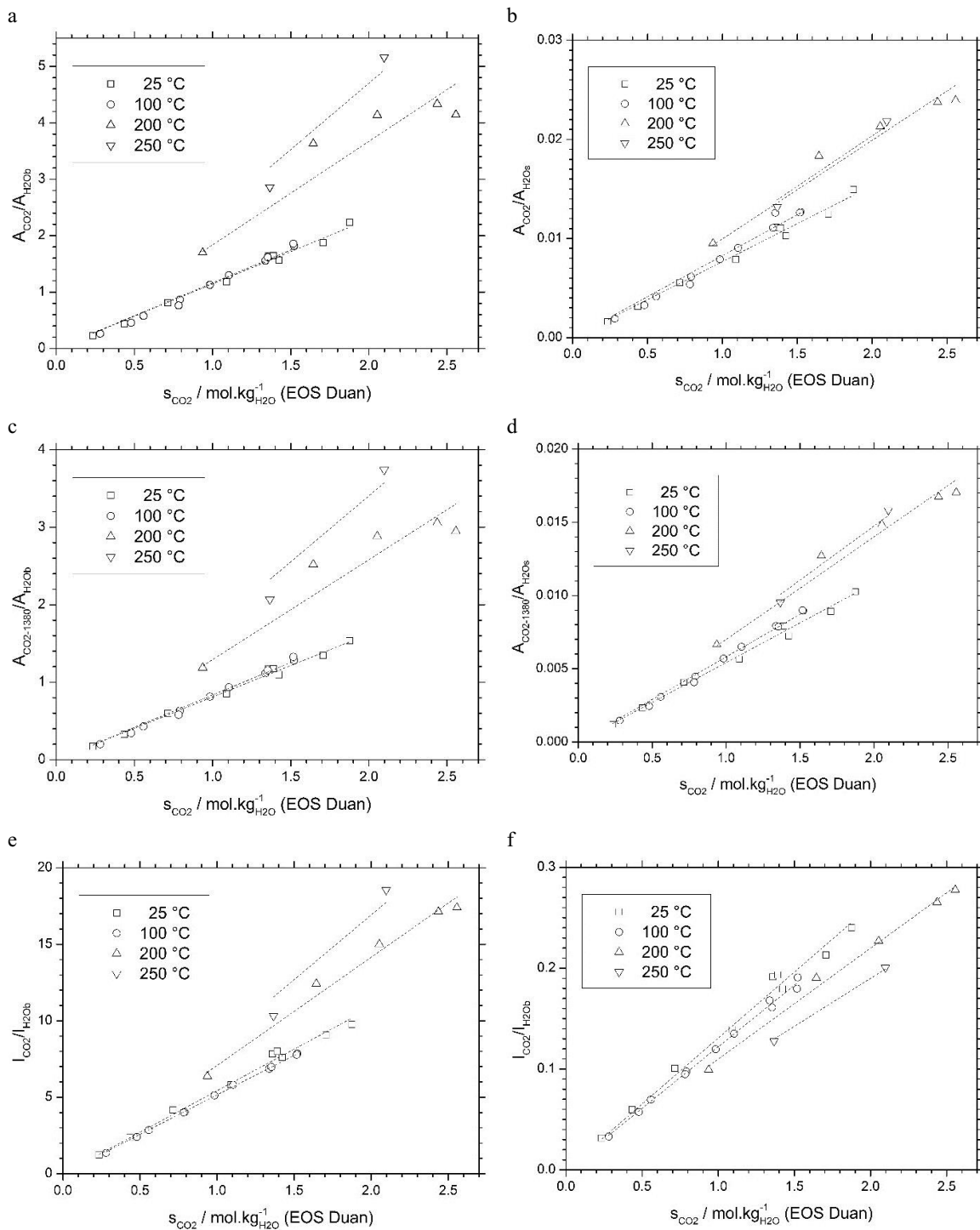


Fig. 6: peak area and peak intensity ratios as a function CO<sub>2</sub> solubility and temperature in pure water. (a)  $A_{CO_2}/A_{H_2Ob}$ , (b)  $A_{CO_2}/A_{H_2Os}$ , (c)  $A_{CO_2-1380}/A_{H_2Ob}$ , (d)  $A_{CO_2-1380}/A_{H_2Os}$ , (e)  $I_{CO_2}/I_{H_2Ob}$ , (f)  $I_{CO_2}/I_{H_2Os}$ . Pressure: 3-500 bar

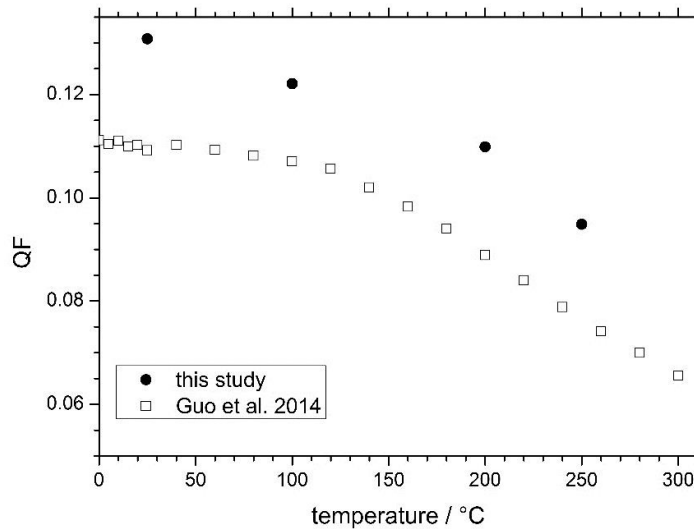


Fig. 7: QF (= to  $(I_{\text{CO}_2}/I_{\text{H}_2\text{O}})/s_{\text{CO}_2}$ ) as a function of temperature in pure water. Comparison of this study (Fig. 6f) with the study of Guo et al. [2].

#### 4. Conclusion

Microcapillaires, connected to a pressurization device, have been used to determine  $\text{CO}_2$  solubility in saline water at 25 °C in the range 0–4 M NaCl, and in pure water as a function of temperature in the range 25 °C–250 °C. This device makes possible fast and reproducible measurements, in a large range of pressure, temperature and salinity that covers the range of interest of  $\text{CO}_2$  geological storage.

The linearity of the response as a function of salinity, whatever which ratio is calculated (intensity or area, to the bending or stretching vibration band of water), confirms the validity of the equation of state of Duan and Sun [1] in this range of experiment (25 °C, 0–4 M NaCl).

#### Acknowledgements

This work was supported by the ANR grant CGS $\mu$ Lab (CGS $\mu$ Lab-ANR-12-SEED-0001).

#### References

- [1] Duan, Z., Sun, R., 2003. An improved model calculating  $\text{CO}_2$  solubility in pure water and aqueous NaCl solutions from 273 to 533 K and from 0 to 2000 bar. *Chem. Geol.*, 2003, **193**, 257–271.
- [2] Guo, H., Chen, Y., Hu, Q., Lu, W., et al., 2014. Quantitative Raman spectroscopic investigation of geo-fluids high-pressure phase equilibria: Part I. Accurate calibration and determination of  $\text{CO}_2$  solubility in water from 273.15 to 573.15 K and from 10 to 120 MPa. *Fluid Phase Equilibria*, 2014, **382**, 70–79.
- [3] Caumon, M.-C., Sterpenich, J., Randi, A., Pironon, J., 2016. Measuring mutual solubility in the  $\text{H}_2\text{O}$ – $\text{CO}_2$  system up to 200 bar and 100 °C by in situ Raman spectroscopy. *Int. J. Greenh. Gas Control*, 2016, **47**, 63–70.
- [4] Chou, I.M., Burruss, R.C., Lu, W., 2005. In: Chen, J, Wang, Y, Duffy, TS, Shen, G, Dobrzynetska, LF (Eds.), *Adv. High-Press. Technol. Geophys. Appl.*, Elsevier, Amsterdam, pp. 475–485.
- [5] Caumon, M.-C., Robert, P., Laverret, E., Tarantola, A., et al., 2014. Determination of methane content in NaCl– $\text{H}_2\text{O}$  fluid inclusions by Raman spectroscopy. Calibration and application to the external part of the Central Alps (Switzerland). *Chem. Geol.*, 2014, **378–379**, 52–61.
- [6] Baonza, V.G., Rull, F., Dubessy, J., 2012. In: Dubessy, J, Caumon, M-C, Rull, F (Eds.), *Raman Spectrosc. Appl. Earth Sci. Cult. Herit.*, vol. 12, The European Mineralogical Union and the Mineralogical Society of Great Britain, London, pp. 279–320.